Supporting Information for "Rapid geomagnetic variations during HSS/SIR, ICME sheath and magnetic cloud-driven geomagnetic storms"

M. N. Pedersen[1], L. Juusola[2], H. Vanhamäki[1], A. T. Aikio[1], A. Viljanen[2]

[1]Space Physics and Astronomy Research Unit, University of Oulu, Oulu, Finland

[2]Finnish Meteorological Institute, Helsinki, Finland

Contents of this file

1. Description of Datasets 1 and 2
2. Description of Figures S1 to S5
3. Figures S1 to S5

Additional Supporting Information (Files uploaded separately)

1. Dataset 1 - Catalog of geomagnetic storms, their phases and solar wind drivers from January 1996 to June 2023
2. Dataset 2 - Geomagnetic storms and their phases from 1981 to 2024

Description of Dataset 1. Text file containing 755 geomagnetic storms, their phases and the solar wind drivers from January 1996 to June 2023. The storms detected are cross-referenced with the ICME catalog by Cane & Richardson (2003) and the HSS/SIR catalog by Grandin et al. (2019) to find the interplanetary drivers at Earth during the geomagnetic storms, as explained in Section 2 of the article. If there are multiple solar wind drivers during a single storm, they are listed in separate rows, in sequential order based on the arrival time of the solar wind driver. In these cases a single storm encompasses several rows in the list, which can be seen from the repeating storm number. This is necessary to accurately display the times of active drivers, as during some storms there may be several separate occurrences of the same driver type (e.g. if two ICMEs reach Earth in short succession, a sheath may be active during the beginning and end of a storm, with an MC or ejecta in between).

As was mentioned in Section 2.3, Cane & Richardson (2003) ICME list occasionally reports a new disturbed region before the end of an already ongoing ejecta. Dataset 1 reports both ICME drivers at the times the ICME catalog has overlapping structures, but in our study, we categorize those times as being driven by the newly arrived sheath region. The following storms have more than 20% of the main phase with sheath and MC overlap: 42, 151, **194**, **195**, **224**, 240, 262, 411, 555 and **664**. The storm numbers in **bold** have 100% overlap during the main phase.

If no driver is reported for a given storm then Cane & Richardson (2003) did not report an ICME nor did Grandin et al report an HSS/SIR at any time during that storm.

Description of Dataset 2. List of geomagnetic storms and phases from the introduction of the SYM-H index in 1981 until 2024. This list does not show the interplanetary drivers, only the storms and storm phases, because Grandin et al. (2019) HSS/SIR and Cane & Richardson (2003) ICME catalogs are only available for the years after 1996.

Figure S1. UT distribution of geomagnetic storms at (left) the time of the SSC, (middle) main phase onsets and (right) recovery phase onsets. The drivers are sorted based on the active interplanetary driver at the sorting time, i.e. for the middle panel it is the active driver at the time of the main phase onset.

Figure S2. Figure S2 shows the total number of storms contributing to each bin for the MLT versus storm-phase-percentage (SPP) analysis. Most of the bins for the main and recovery phases have contributions from more than 20 different storms, with the fewest found in the end of the recovery phase for sheath storms. The SSC and initial phase generally have fewer storms contributing to each bin. For the HSS/SIR storms there are always more than 3 storms contributing to each bin, and for sheath there are always more than 10 storms. The fewest are for MCs in the SSC and early initial phase.

Figure S3. Polar figure showing the number of different geomagnetic storms contributing to the MLT-MLAT bins for the three solar wind driver categories during the SSC, main phase and recovery phase. The main and recovery phases have more than 30 storms contributing to each bin, except during sheath storms at three latitude circles. Those three latitude circles have fewer storms in all categories. It's because those bins only had one or two stations contributing to it that became operational in the middle of the study or that the movement of the geomagnetic pole shifted station coverage of the bins at some point during the study. Particularly, in the top latitude circle (76.5-78 MLAT) it is because NAL station moved into that bin after 2008, as the only station contributing to it. The middle latitude circle (72-73.5 MLAT) HOP station moved out of the bin after 2008, and for the lower latitude circle (67.5-69 MLAT) SOR moved into it after 2008 and NOR became operational in late 2007, which are the only contributors to the bin. For

the SSC, fewer storms contribute to each bin, as the SSC only lasts 10 min; from 2 min before the sudden impulse until 5 min after the impulse.

Figure S4. Total number of 10 s measurements from all the IMAGE stations in each of the MLT versus storm-phase percentage (SPP) bin. Some MLT dependence can be seen in the main and recovery phase following the UT dependence of geomagnetic storms that was observed in Figure S1.

Figure S5. Total number of 10 s measurements from all the IMAGE stations in each of the MLT versus MLAT bins.

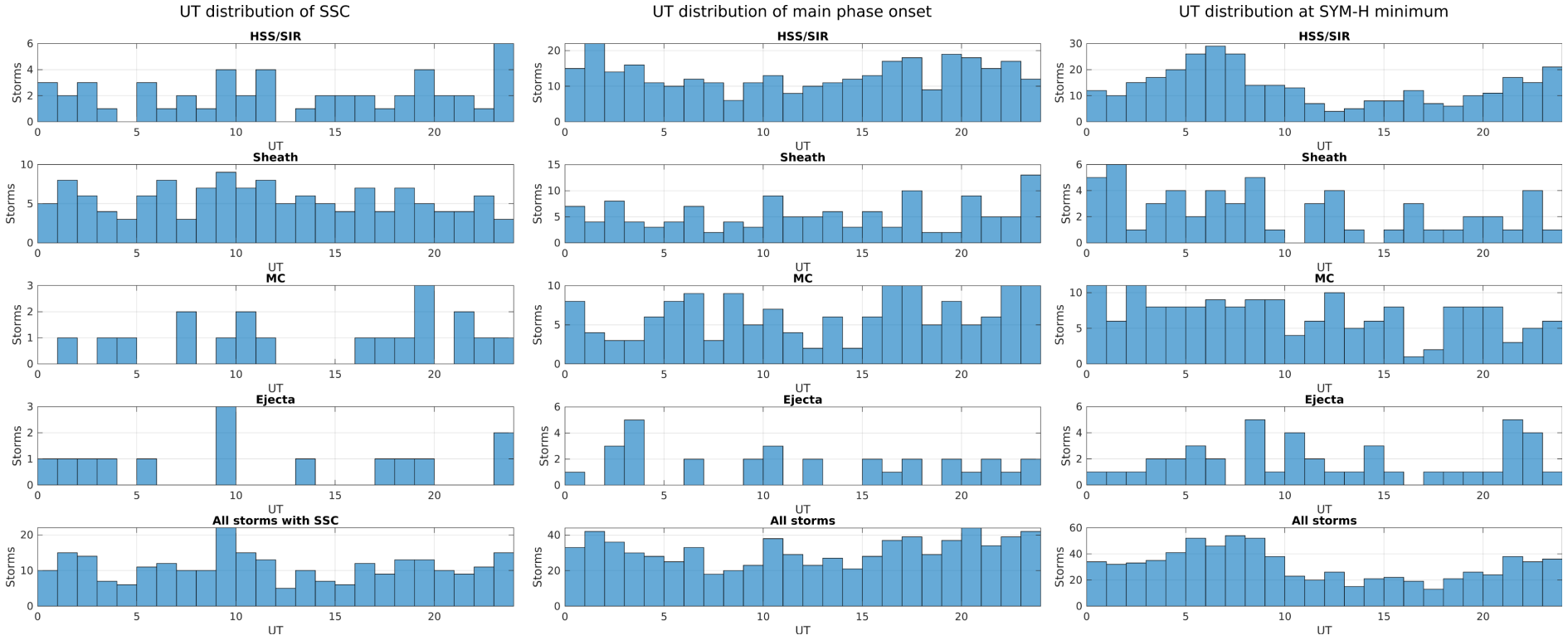

Figure S1. UT distribution of geomagnetic storms when the active driver is HSS/SIR, sheath, MC, ejecta or all drivers from top to bottom, respectively. The left side shows the UT distribution of the main phase onset times and on the right side is the UT distributions at the time of SYM-H index minimum (recovery phase onset times).

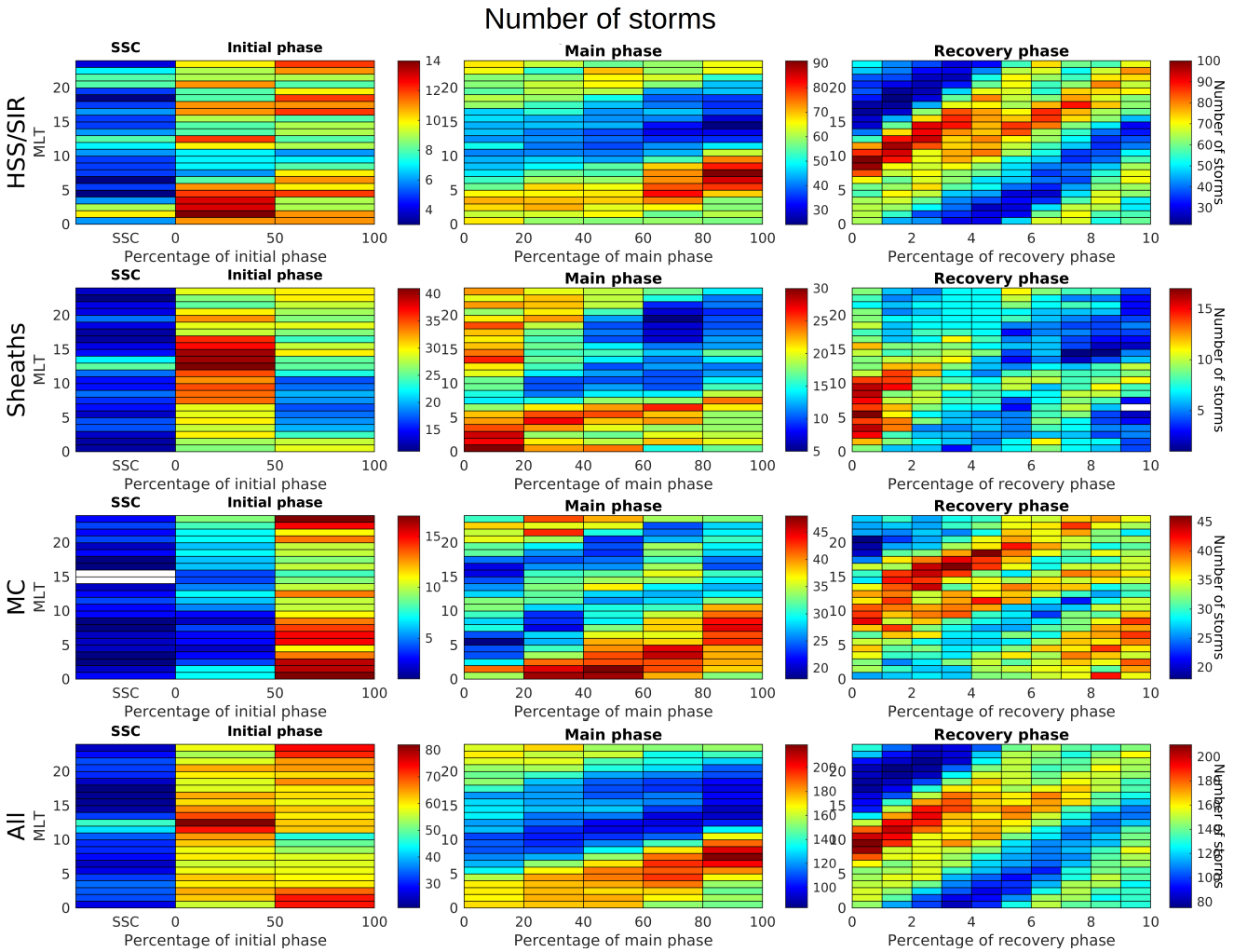

Figure S2. Number of different geomagnetic storms with measurements in each bin. Fewer storms contribute to the SSC bin as it is only 10 min.

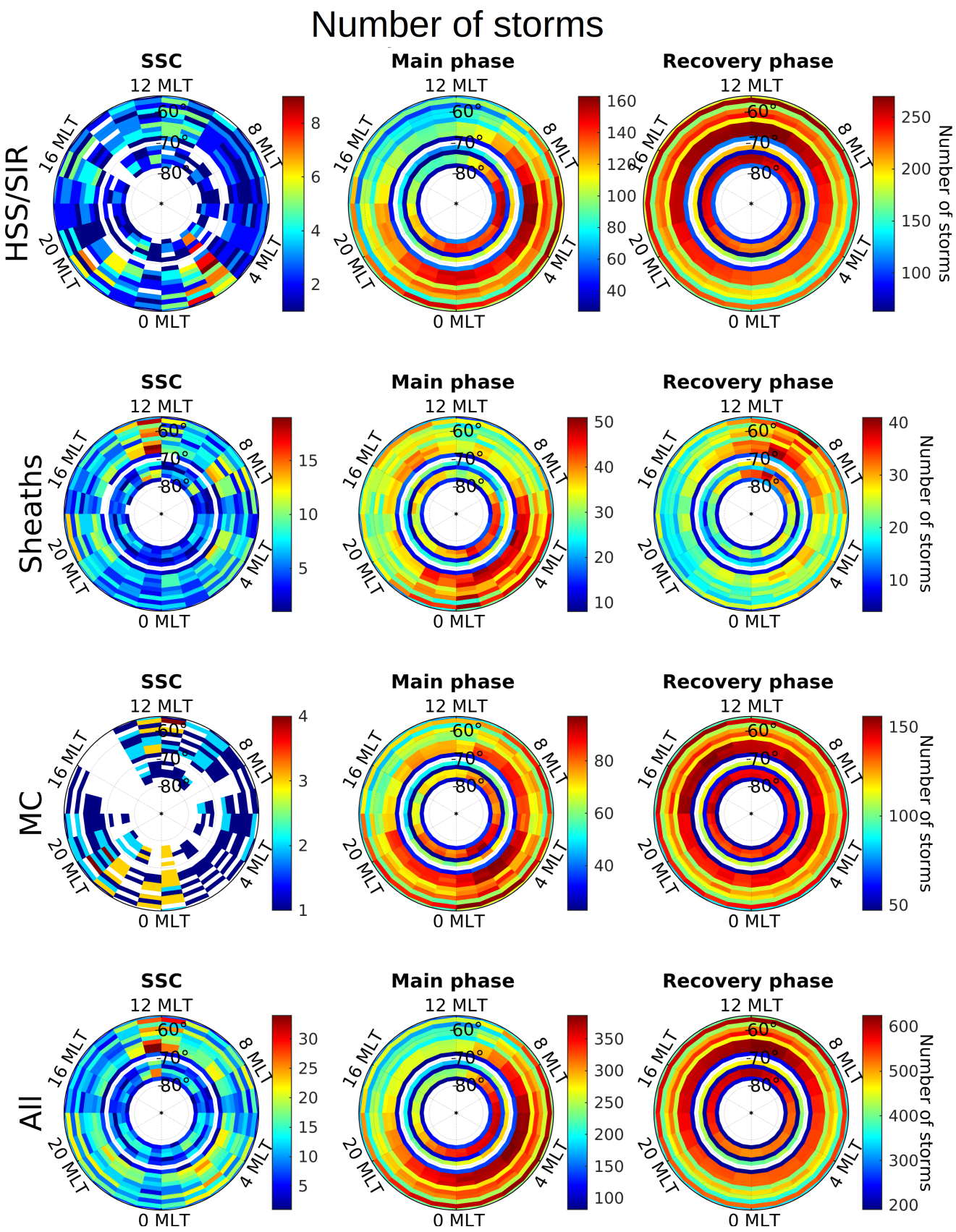

Figure S3. Number of different geomagnetic storms with measurements in each bin.

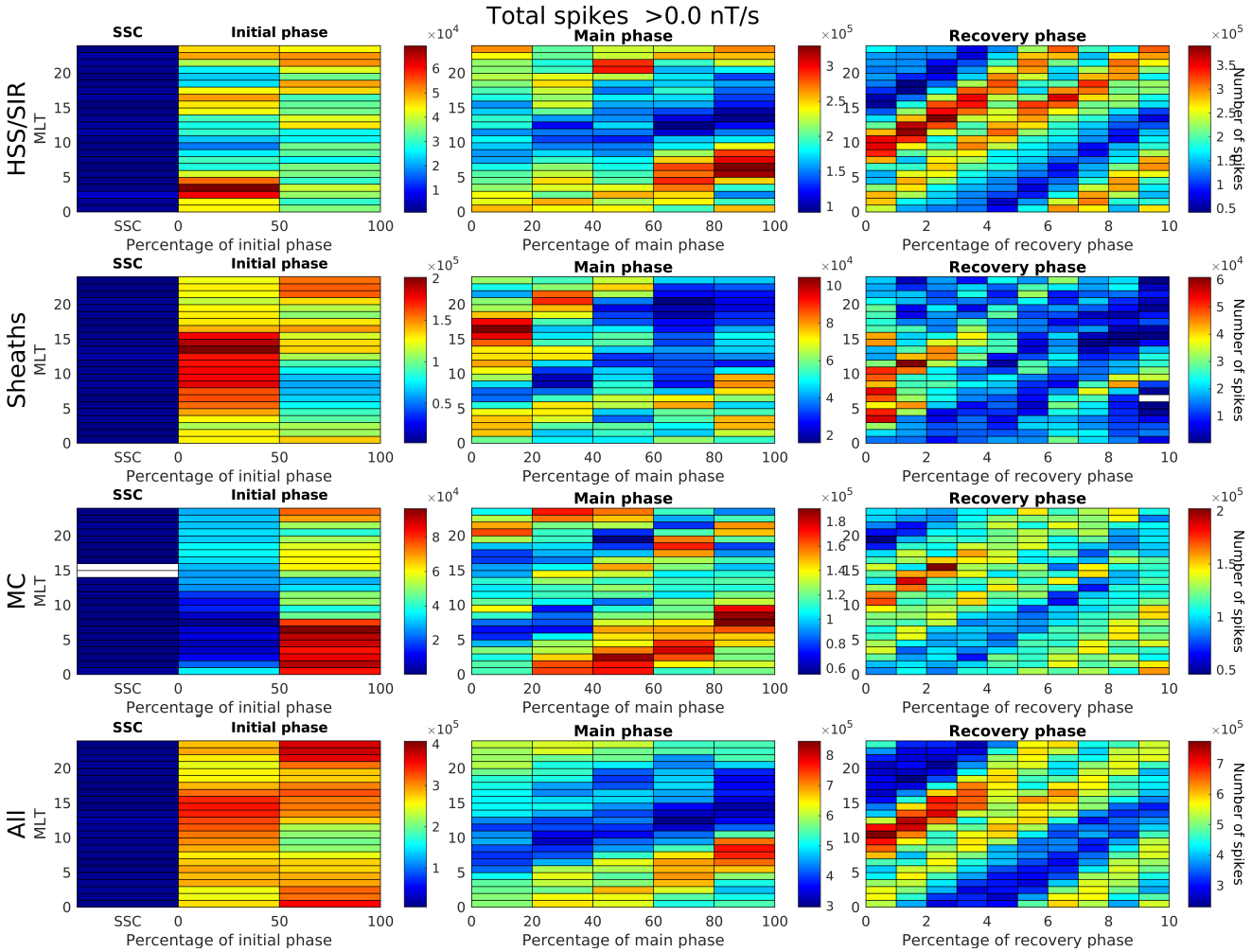

Figure S4. Total number of measurements in each bin. This cell is used to normalize the number of counts in each bin that is used to get the probabilities in Figure 6 of the article.

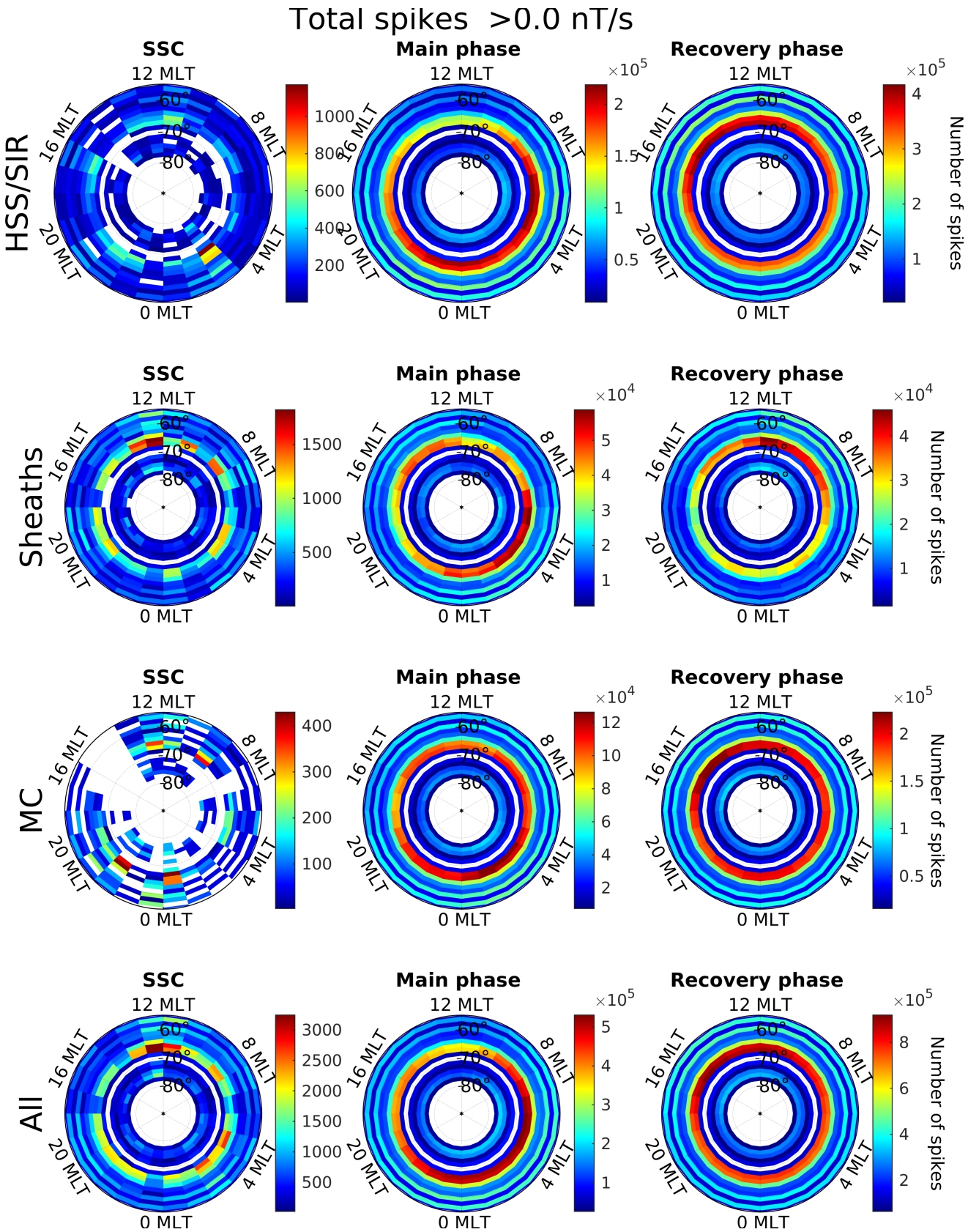

Figure S5. Total number of measurements in each bin. This cell is used to normalize the number of counts in each bin that is used to get the probabilities in Figure 7 of the article.